# Sensitive characterization of phase and amplitude semiconductor nonlinearities for broadband 20 fs excitation

J. Kunde,[a] S. Arlt, L. Gallmann, F. Morier-Genoud, U. Siegner, and U. Keller
*Ultrafast Laser Physics, Institute of Quantum Electronics, Swiss Federal Institute of Technology Zurich, ETH Hoenggerberg-HPT, CH-8093 Zurich, Switzerland*

(Received 20 September 1999; accepted for publication 12 April 2000)

We present an experimental technique that allows for the detection of pump-induced transmission and phase changes with high sensitivity and ultrafast temporal resolution over an arbitrarily wide time window. This is achieved combining spectral interferometry with high-frequency-chopping differential transmission measurements. With this setup, exciton and continuum nonlinearities in a semiconductor are studied for broadband excitation. We find that the pump-induced phase changes at the exciton and in the continuum decay on distinctly different time scales, indicating different microscopic origins. © *2000 American Institute of Physics.* [S0021-8979(00)04514-X]

With the advent of Ti:sapphire lasers, pulses as short as only a few optical cycles became available at a repetition rate of about 100 MHz.[1] These sources are ideally suited for ultrafast, spectrally broadband spectroscopic investigations. The high repetition rates allow for differential transmission (DT) measurements using chopping frequencies in the MHz range where laser noise is significantly reduced as compared to the kHz range.[2] In this way, the sensitive measurement of small optical nonlinearities becomes feasible at low to moderate excitation levels. In DT experiments, only the amplitude of the probe field is analyzed. However, the optical phase may give additional insight into the microscopic physics in various materials, e.g., in semiconductors.[3–6] Spectrally integrated (SI) phase changes can be measured with high sensitivity using time division interferometry.[7,8] An elegant way to sensitively measure small, spectrally resolved (SR) phase changes in a weak broadband optical pulse is the usage of spectral interferometry. Its implementation in a DT setup has been demonstrated, e.g., in Refs. 9–11. Those experimental setups did not take advantage of the substantial improvement of the DT sensitivity which could be obtained using chopping techniques and lock-in detection. In particular, the advantages of high-frequency (HF) chopping could not be exploited since laser systems were used with repetition rates of only 10 kHz or below. In this communication, we experimentally demonstrate how spectral interferometry can be implemented in a DT setup with 20 fs time resolution and high DT sensitivity given by HF chopping and lock-in detection. In our setup, phase dynamics can be studied in a temporal window limited only by the repetition rate of the laser, in contrast to earlier work.[9–11] The setup presented in this letter provides a versatile tool for the study of phase dynamics in various materials.

With this setup, we have studied phase and amplitude semiconductor nonlinearities for broadband excitation of excitonic and continuum transitions. So far, measurements of phase dynamics in semiconductors have concentrated on excitonic excitations.[3–5] However, the broadband amplitude and phase continuum nonlinearities will become increasingly important for future semiconductor switching devices operating on the 10 fs time scale. Our data show that higher-order phase changes in the semiconductor continuum and at the exciton decay on strikingly different time scales. This demonstrates that they have different physical origins. While the decay of the excitonic phase changes can be attributed to the lifetime of carriers in a thermalized distribution, the decay of the phase change in the continuum is determined by thermalization or dephasing processes.

In our experimental setup shown in Fig. 1, we use 20 fs pulses from a Ti:Sapphire oscillator operating at 90 MHz repetition rate. After dispersion precompensation, beam splitter BS 1 splits the pump pulse from the probe and the reference. To implement HF chopping without the excessive dispersion inherent in acousto-optical modulators, we use a mechanical chopper in the pump beam, which allows for chopping frequencies up to 1 MHz. A small portion of the modulated pump serves as reference signal for the HF lock-in amplifier. The probe/reference beam is chopped at a few 100 Hz. BS 3 splits the probe from the reference pulse. The latter is needed for spectral interferometry. Note that the reference pulse does not propagate through the sample, in contrast to earlier work.[9–11] If the reference pulse passes through the sample, it has to arrive at the sample prior to the pump pulse since the pump should only influence the transmission of the probe pulse. This requirement restricts the pump-probe delay to values smaller than the probe-reference delay, which is limited by the finite spectral resolution of the interferogram detection. For example, the delays were restricted to a few hundreds of femtoseconds in Refs. 9–11. Our setup circumvents this limitation, as suggested in Ref. 10.

BS 4 directs part of the probe to the photodiode PD 2 for DT detection. The SI DT or the SR DT is detected with cascaded lock-in amplifiers. For the acquisition of the SR DT, a scanning monochromator is used. Combined with HF chopping, we have found this scanning scheme to be more sensitive than the acquisition of the whole spectrum with a

[a]Electronic mail: kunde@iqe.phys.ethz.ch

 

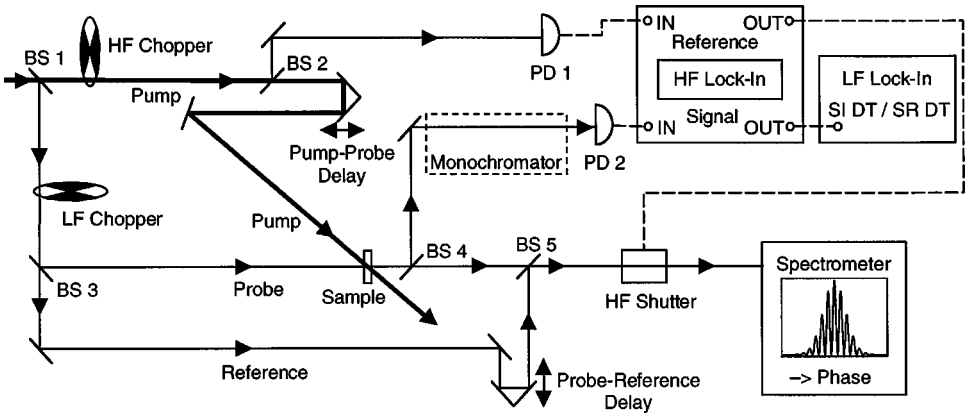


FIG. 1. Schematic of the experimental setup for the sensitive measurement of spectrally integrated (SI) differential transmission (DT), spectrally resolved (SR) DT, and pump-induced phase changes. BS: beam splitter. HF: high frequency. PD: photodiode. The low-frequency (LF) chopper provides the reference for the LF lock-in. Solid lines: optical beam path. Dashed lines: electrical connections.

multichannel detector in the absence and presence of the pump at relatively low rates. BS 5 recombines the probe and the reference pulse. An acousto-optic modulator is used as a HF shutter in front of the spectrometer. This shutter is synchronized with the HF chopper in the pump via the HF lock-in. The shutter guarantees that the interferogram is acquired only during pump excitation of the sample. Without this shutter, the interferogram would be averaged over pump-on and pump-off conditions, making the extraction of the pump-induced phase changes difficult. Note that the HF chopper should be kept in the pump beam during measurements of interferograms. This ensures that phase and DT data are acquired with the same average laser power and the same thermal load on the sample.

To demonstrate the capabilities of the setup, we have studied a 1 $\mu$m thick $Al_{0.06}Ga_{0.94}As$ bulk semiconductor sample. The pulse spectrum spans from the band edge to states high up in the band [see inset of Fig. 2(b)]. All experiments were performed at room temperature. In the inset of Fig. 2(a), a SI DT curve is shown for very low carrier density and an acquisition time of 1 s per data point. The curve shows that normalized transmission changes $\Delta T/T$ of about $10^{-6}/\sqrt{\text{Hz}}$ can be measured with the HF chopping technique. If high sensitivity is not needed, the setup allows for the fast acquisition of large data sets.[12] The SR DT data in Fig. 2(b) and the phase data in Fig. 3 have been taken at the higher carrier density $N_{\text{exc}} \approx 5\times10^{17}\,\text{cm}^{-3}$. The SR DT data show the well-known dynamics of nonequilibrium carrier distributions in the thermalization regime.[13] Figure 2(a) shows the SI DT curve taken at the same density. More details will be discussed later.

The standard spectral interferometry algorithm[14] allows for the retrieval of the relative phase $\phi_{\text{rel}}$ between reference and probe pulse:

$$\phi_{\text{rel}}(\omega,\tau) = \omega\,\theta(\tau) + \varphi(\omega,\tau). \tag{1}$$

For an angular frequency $\omega_0$, $\theta$ denotes the delay by which the probe precedes the reference pulse and $\varphi$ is the phase difference between probe and reference in higher than linear order in $(\omega-\omega_0)$. An increase in the refractive index of the sample corresponds to a decrease in $\phi_{\text{rel}}$. $\theta$ and $\varphi$ may both change as functions of the pump-probe delay $\tau$ due to pump-induced phase changes. $\theta$ may also change due to fluctuations $\delta\theta$ in the probe-reference delay, i.e., due to instabilities of the setup. We have found that $\theta$ fluctuates by about $\delta\theta \approx 0.15$ fs over half an hour. This allows for measurements of pump-induced changes in the linear phase term $(\omega-\omega_0)\theta$ as small as, e.g., 0.024 rad between 750 and 800 nm. $\delta\theta$ does not influence $\varphi$. Therefore, even smaller higher-order phase changes can be accurately measured without the need of active interferometric stabilization. While pump-induced changes in $\theta$ modify the arrival time of the probe pulse,

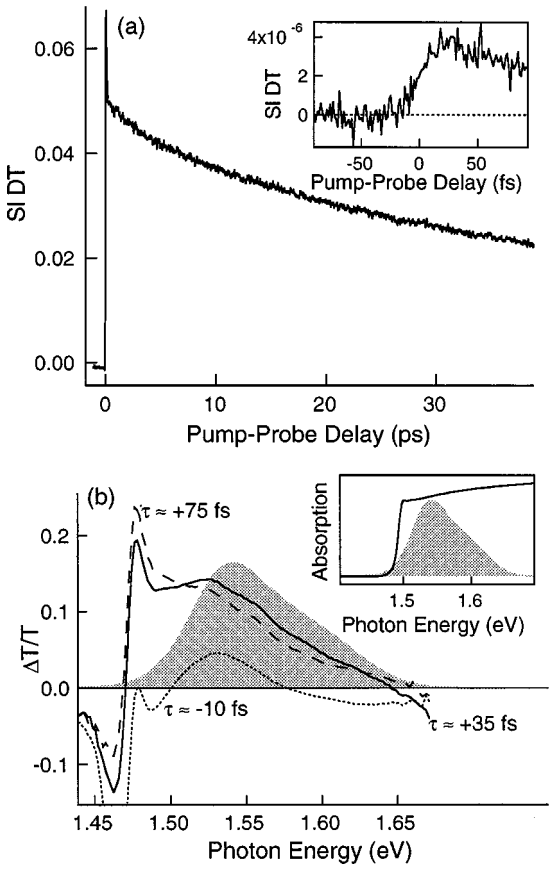


FIG. 2. (a) Spectrally integrated differential transmission (SI DT) and DT spectra (b) for three different pump-probe delays $\tau$. Pump and probe are linearly cross polarized. Carrier density: $N_{\text{exc}} \approx 5\times10^{17}\,\text{cm}^{-3}$. Shaded: excitation pulse spectrum. Inset of (a): SI DT for a reduced carrier density. Inset of (b): room temperature linear absorption spectrum of the $Al_{0.06}Ga_{0.94}As$ bulk semiconductor sample and excitation pulse spectrum (shaded).

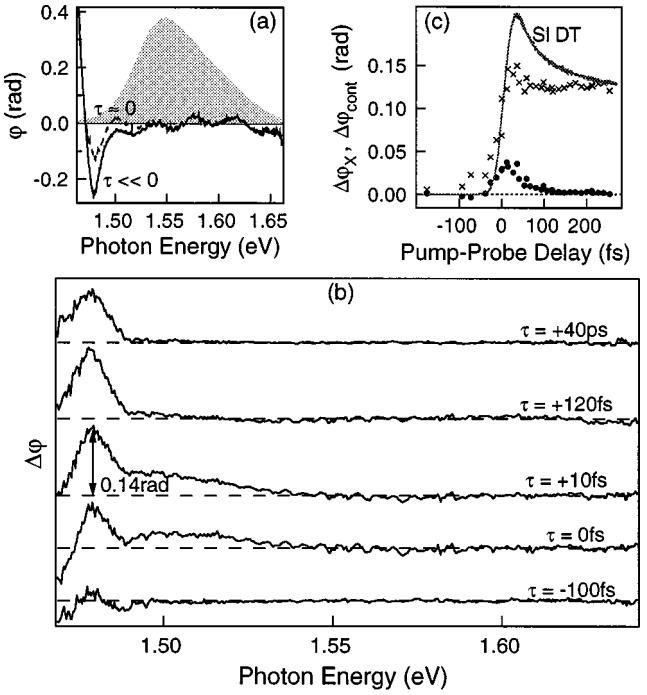


FIG. 3. (a) Higher-order probe-reference phase difference $\varphi$ for two different pump-probe delays $\tau$. Shaded: Excitation pulse spectrum. (b) Pump-induced phase changes $\Delta\varphi$ for five delays $\tau$. (c) Pump-induced phase changes at the exciton $\Delta\varphi_X$ (crosses) and in the continuum $\Delta\varphi_{\mathrm{cont}}$ (circles) versus pump-probe delay. Carrier density: $N_{\mathrm{exc}} \approx 5\times 10^{17}\,\mathrm{cm}^{-3}$. Also shown: spectrally integrated differential transmission (SI DT).

pump-induced changes of the higher-order phase term $\varphi$ modify the temporal shape of the probe pulse. In the following, we will focus on $\varphi$, which contains substantial physics.

Figure 3(a) shows $\varphi$ for two pump-probe delays ($\hbar\omega_0 = 1.57\,\mathrm{eV}$). For large negative pump-probe delays, the pump changes the probe only due to thermal effects but not due to interband excitation. The shape of $\varphi$ close to the exciton resonance qualitatively reproduces the higher-order terms in the linear refractive index of direct-bandgap semiconductors.[15] This indicates that, without the sample, higher-order phase terms are well balanced between both interferometer arms.[16] For pump-probe delays approaching $\tau \approx 0$, the pump changes $\varphi$ due to interband excitation. To extract these changes, $\Delta\varphi = \varphi(\tau) - \varphi(\tau \ll 0)$ is plotted for several pump-probe delays $\tau$ in Fig. 3(b). An analysis of the noise shows that $\Delta\varphi(\omega, \tau)$ can be measured with a sensitivity of better than 0.01 rad. Two main contributions to $\Delta\varphi$ can be seen: (*i*) $\Delta\varphi_X$, at the excitonic resonance at about 1.48 eV, and (*ii*) $\Delta\varphi_{\mathrm{cont}}$, in the semiconductor continuum between 1.49 eV up to about 1.54 eV.

Figure 3(c) shows the changes of these contributions with pump-probe delay. The phase changes at the exciton build up as the SI DT, determined by the pulse width. The subsequent decay of $\Delta\varphi_X$ [Figs. 3(b), and 3(c)] has a time constant of about 50 ps. This is the lifetime of the thermalized carrier distribution, as measured in SI DT [see Fig. 2(a)]. Therefore, we conclude that the thermalized carrier distribution causes the phase changes at the exciton. The temporal shape of the probe pulse is modified due to $\Delta\varphi_X$ as long as carriers are present. These carriers broaden the exciton resonance, which leads to phase changes, as observed earlier.[6] Moreover, the carriers weaken the oscillator strength of the excitonic resonance due to phase space filling and screening, resulting in additional phase changes. The same effects are reflected in the SR DT [see Fig. 2(b)].

The higher-order phase changes $\Delta\varphi_{\mathrm{cont}}$ in the semiconductor continuum decay with a sub-100-fs time constant, i.e., much faster than $\Delta\varphi_X$ [Figs. 3(b) and 3(c)]. This shows that the continuum phase changes have a different physical origin. We recall that the carrier distributions thermalize in about 100 fs, as shown in Fig. 2(b). The comparison of the time constants demonstrates that higher-order continuum phase changes are only caused by *nonthermal* carrier distributions or coherent effects. This suggests that a spectrally well-localized perturbance of the flat continuum is required to produce higher-order phase changes. Our results are in line with quasi-steady-state studies which showed that the total pump-induced refractive index changes were spectrally flat.[17]

In summary, we have presented a setup that allows for the measurement of broadband nonlinear amplitude and phase dynamics with high sensitivity and 20 fs time resolution over a wide temporal window. This setup has allowed us to identify distinctly different time constants for the phase dynamics in the semiconductor continuum and at the exciton.

The authors would like to thank D. J. Hagan and G. Steinmeyer for helpful discussions. This work has been supported by the Swiss National Science Foundation.

[1] G. Steinmeyer, D. H. Sutter, L. Gallmann, N. Matuschek, and U. Keller, Science **286**, 1507 (1999).
[2] A. Poppe, L. Xu, F. Krausz, and C. Spielmann, IEEE J. Sel. Top. Quantum Electron. **4**, 179 (1998).
[3] D. S. Chemla, J.-Y. Bigot, M.-A. Mycek, S. Weiss, and W. Schäfer, Phys. Rev. B **50**, 8439 (1994).
[4] G. Böhne, S. Freundt, S. Arlt, D. Pfister, C. Nacke, J. S. Nägerl, and R. G. Ulbrich, Phys. Status Solidi B **188**, 321 (1995).
[5] H. Giessen, S. Linden, J. Kuhl, A. Knorr, S. W. Koch, F. Gindele, M. Hetterich, M. Grün, S. Petillon, C. Klingshirn, and N. Peyghambarian, Phys. Status Solidi B **206**, 27 (1998).
[6] J. Tignon, M. V. Marquezini, T. Hasche, and D. S. Chemla, IEEE J. Quantum Electron. **35**, 510 (1999).
[7] K. L. Hall, A. M. Darwish, E. P. Ippen, U. Koren, and G. Raybon, Appl. Phys. Lett. **62**, 1320 (1993).
[8] D. H. Hurley and O. B. Wright, Opt. Lett. **24**, 1305 (1999).
[9] E. Tokunaga, A. Terasaki, and T. Kobayashi, Opt. Lett. **17**, 1131 (1992).
[10] E. Tokunaga, A. Terasaki, and T. Kobayashi, J. Opt. Soc. Am. B **12**, 753 (1995).
[11] J. P. Geindre, P. Audebert, A. Rousse, F. Falliès, J. C. Gauthier, A. Mysyrowicz, A. Dos Santos, G. Hamoniaux, and A. Antonetti, Opt. Lett. **19**, 1997 (1994).
[12] J. Kunde, U. Siegner, S. Arlt, G. Steinmeyer, F. Morier-Genoud, and U. Keller, J. Opt. Soc. Am. B **16**, 2285 (1999).
[13] J. Shah, *Ultrafast spectroscopy of semiconductors and semiconductor nanostructures*, 2nd ed. (Springer-Verlag, Berlin, 1999).
[14] L. Lepetit, G. Chériaux, and M. Joffre, J. Opt. Soc. Am. B **12**, 2467 (1995).
[15] C. Tanguy, IEEE J. Quantum Electron. **32**, 1746 (1996).
[16] The small residual oscillations show that this balancing was not perfect.
[17] Y. H. Lee, A. Chavez-Pirson, S. W. Koch, H. M. Gibbs, S. H. Park, J. Morhange, A. Jeffery, N. Peyghambarian, L. Banyai, A. C. Gossard, and W. Wiegmann, Phys. Rev. Lett. **57**, 2446 (1986).